

AD-A203 173

APPROVED FOR PUBLIC RELEASE;
DISTRIBUTION UNLIMITED

69 1-08-184

UNCLASSIFIED

SECURITY CLASSIFICATION OF THIS PAGE

REPORT DOCUMENTATION PAGE

1a. REPORT SECURITY CLASSIFICATION Unclassified		1b. RESTRICTIVE MARKINGS	
2a. SECURITY CLASSIFICATION AUTHORITY		3. DISTRIBUTION / AVAILABILITY OF REPORT Approved for public release; distribution unlimited.	
2b. DECLASSIFICATION / DOWNGRADING SCHEDULE		4. PERFORMING ORGANIZATION REPORT NUMBER(S) TR-0088(3945-07)-5	
4. PERFORMING ORGANIZATION REPORT NUMBER(S) TR-0088(3945-07)-5		5. MONITORING ORGANIZATION REPORT NUMBER(S) SD-TR-88-102	
6a. NAME OF PERFORMING ORGANIZATION The Aerospace Corporation Laboratory Operations	6b. OFFICE SYMBOL (If applicable)	7a. NAME OF MONITORING ORGANIZATION Space Division	
6c. ADDRESS (City, State, and ZIP Code) El Segundo, CA 90245		7b. ADDRESS (City, State, and ZIP Code) Los Angeles Air Force Base Los Angeles, CA 90009-2960	
8a. NAME OF FUNDING / SPONSORING ORGANIZATION	8b. OFFICE SYMBOL (If applicable)	9. PROCUREMENT INSTRUMENT IDENTIFICATION NUMBER F04701-85-C-0086-P00019	
8c. ADDRESS (City, State, and ZIP Code)		10. SOURCE OF FUNDING NUMBERS	
		PROGRAM ELEMENT NO.	PROJECT NO.
		TASK NO.	WORK UNIT ACCESSION NO.
11. TITLE (Include Security Classification) Distribution of Boron Atoms in Ion Implanted Compound Semiconductors			
12. PERSONAL AUTHOR(S) Bowman, R. C. Jr. and Knudsen, J. F. (The Aerospace Corporation) Downing, R. G. (National Bureau of Standards) and Kremer, R. E. (Oregon Graduate Center)			
13a. TYPE OF REPORT	13b. TIME COVERED FROM TO	14. DATE OF REPORT (Year, Month, Day) 1988 November 25	15. PAGE COUNT
16. SUPPLEMENTARY NOTATION			
17. COSATI CODES		18. SUBJECT TERMS (Continue on reverse if necessary and identify by block number)	
FIELD	GROUP	SUB-GROUP	
		Ion Implanation, Gallium Arsenides, Cadmium telluride, Mercury compounds, Boron. (mg)	
19. ABSTRACT (Continue on reverse if necessary and identify by block number)			
<p>The nondestructive neutron depth profiling (NDP) technique has been used to measure the boron (^{10}B) distributions in GaAs, CdTe, $\text{Hg}_{0.7}\text{Cd}_{0.3}\text{Te}$, and $\text{Hg}_{0.85}\text{Mn}_{0.15}\text{Te}$ after multiple energy ion implants. The NDP results are found to be in good agreement with the theoretical ion ranges obtained from Monte Carlo computer simulations. Only minor changes in the boron profiles were seen for the chosen annealing conditions.</p>			
20. DISTRIBUTION / AVAILABILITY OF ABSTRACT <input checked="" type="checkbox"/> UNCLASSIFIED/UNLIMITED <input type="checkbox"/> SAME AS RPT. <input type="checkbox"/> DTIC USERS		21. ABSTRACT SECURITY CLASSIFICATION Unclassified	
22a. NAME OF RESPONSIBLE INDIVIDUAL		22b. TELEPHONE (Include Area Code)	22c. OFFICE SYMBOL

PREFACE

The technical assistance of Dr. P. M. Adams, R. E. Robertson, Dr. R. J. Kranzt, and G. A. To is greatly appreciated. Certain commercial equipment, instruments, or materials are identified to specify experimental procedures. Such identification does not imply recommendation or endorsement by the National Bureau of Standards.



Accession For	
NTIS GRA&I	<input checked="" type="checkbox"/>
DTIC TAB	<input type="checkbox"/>
Unannounced	<input type="checkbox"/>
Justification	
By _____	
Distribution/	
Availability Codes	
Dist	Avail and/or Special
A-1	

Ion implantation is widely used to fabricate optoelectronic devices from many compound semiconductors. For example, boron ion implants can produce the n-p junctions in $\text{Hg}_{1-x}\text{Cd}_x\text{Te}$ for infrared photovoltaic detectors (Ref.1) or provide isolation of electrically active regions in GaAs microwave devices (Ref.2). Although there have been many studies on boron implantation into silicon, little information is available on the behavior of boron implants in the compound semiconductors (Refs. 3-7). The present work compares the boron profiles for different semiconductors that had been simultaneously implanted with boron ions and assesses the effects of typical process annealing treatments on the boron distributions.

The conditions for the multiple energy implants with the $^{10}\text{B}^+$ isotopes are summarized in Table 1. The ion beams were about 7° off-axis to reduce channeling effects; additional details are given in Refs. 5 and 6. The samples consisted of (100)-GaAs that was undoped and semi-insulating, (100)- and (111)-CdTe crystals from II-VI Incorporated, bulk (100)- and (110)- $\text{Hg}_{0.68}\text{Cd}_{0.32}\text{Te}$ from Cominco, epitaxial (111)- $\text{Hg}_{0.7}\text{Cd}_{0.3}\text{Te}$ from Rockwell, and unoriented $\text{Hg}_{0.85}\text{Mn}_{0.15}\text{Te}$ single crystals grown by a modified Bridgeman method. The average composition for $\text{Hg}_{0.85}\text{Mn}_{0.15}\text{Te}$ was obtained from an X-ray determination of its cubic lattice parameter (i.e., $a = 0.6439 \text{ nm}$) and measured density (7.72 g/cm^3). The boron ions (^{10}B) were implanted into polished faces. Low temperature Hall measurements indicated that boron implants produced degenerate n-type layers in the $\text{Hg}_{0.7}\text{Cd}_{0.3}\text{Te}$ and $\text{Hg}_{0.85}\text{Mn}_{0.15}\text{Te}$ samples, which are similar to previously described observations (Ref. 5).

The neutron depth profiling (NDP) determinations of the ^{10}B distributions from the reaction $^{10}\text{B}(n,\alpha)^7\text{Li}$ were performed with the 20-MW research reactor at the National Bureau of Standards. Most of the NDP procedures have been reported elsewhere (Refs. 5,6). However, to eliminate the "pulse pile-up" effects which asymmetrically broadened the previous NDP profiles for the $\text{Hg}_{1-x}\text{Cd}_x\text{Te}$ samples (Refs. 5,6), fully depleted transmission silicon detectors with nominal $40 \mu\text{m}$ thicknesses have been used for the present NDP experiments and have produced higher resolution profiles with minimal distortions. The NDP results have a 50 nm full-width half-maximum resolution.

Table 1. Summary of Boron Ion (^{10}B) Implant Conditions

Implant Series Label	Nominal Target Temp (K)	Different Ion Energies	Number of Ion Energies (keV)	Dose at Each Energy (10^{15} ions/cm 2)	Ion Beam Current ($\mu\text{A}/\text{cm}^2$)
B	298	2	50	5.0	0.09
			100	10.0	0.12
E	78	4	100	0.5	0.037
			200	0.5	0.044
			300	0.5	0.044
			400	0.5	0.036

The boron distributions for the Type-B implant conditions are presented in Fig. 1, where the NDP results are compared with the theoretical profiles from a TRIM-86 version of the Monte Carlo computational method developed by Biersack et al. (Refs. 8,9). Quite good agreement between the NDP and TRIM profiles are apparent in Fig. 1 for the three distinct materials. However, some minor differences are found at the ends of the ion ranges with the TRIM simulations predicting slightly more shallow profiles. The discrepancies may arise from some channeling contributions or other interactions not included in the TRIM analyses. The behavior of the Type E boron implants into liquid nitrogen cooled crystals is summarized in Fig. 2. The peak boron contents in Fig. 2 are much below those in Fig. 1 since the implant doses for Type E were smaller. Once again the NDP measured profiles are in good agreement with the TRIM calculated ion ranges. The lower target temperatures during Type E implantation should minimize any thermally activated motion of either boron or the implant induced defects. The tendency of the boron peak to occur closer to the surface is also noted in Fig. 2 for both Hg-based crystals. This behavior is attributed to enhanced backscattering of the boron ions during implantation due to the heavier masses of the target atoms as compared to GaAs.

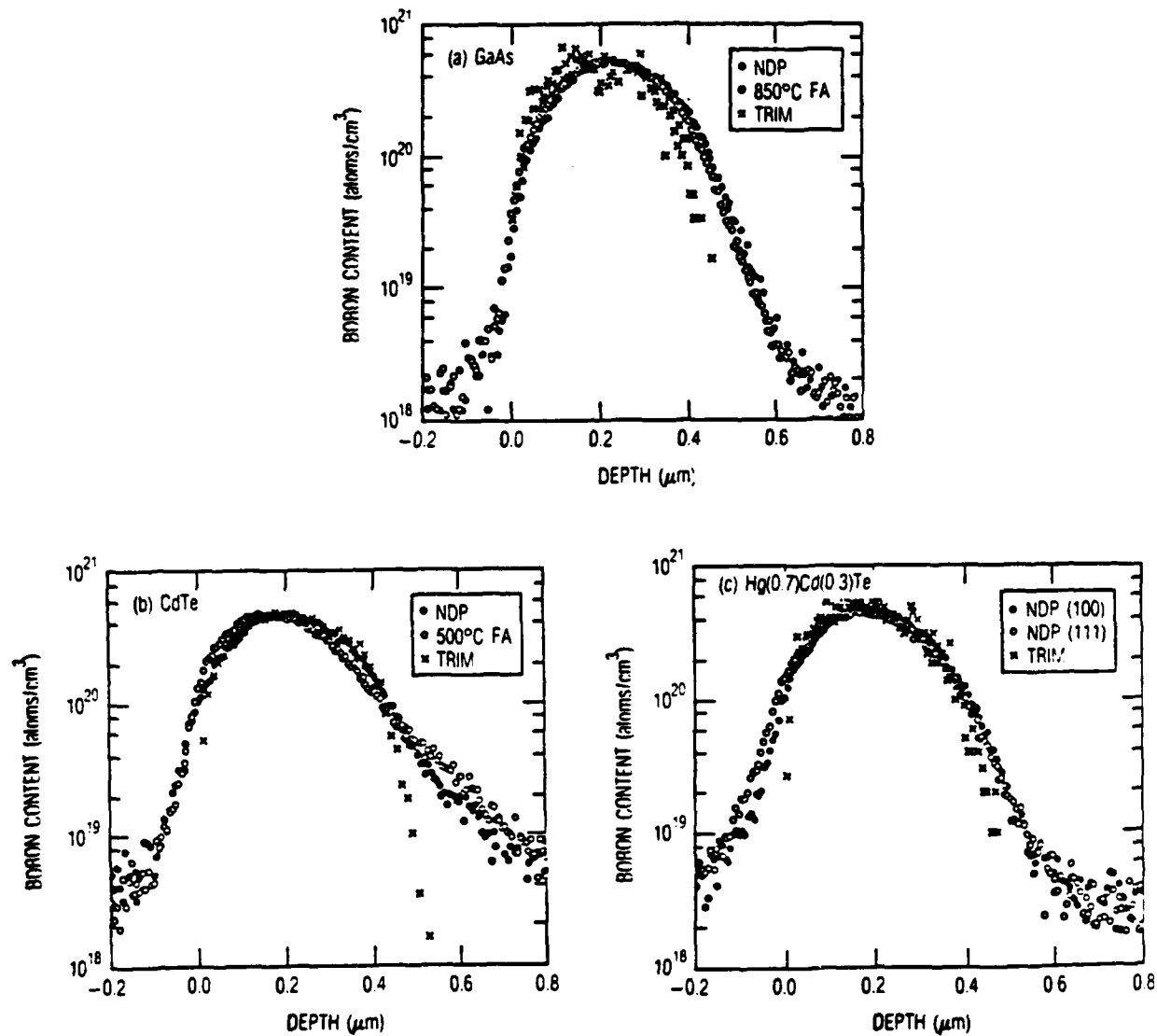


Fig. 1. NDP Profiles from (a) (100)-GaAs, (b) (111)-CdTe, and (c) Hg_{0.7}Cd_{0.3}Te after Type B Boron Ion Implants. The predicted distributions from TRIM Monte Carlo calculations are denoted by "X" points.

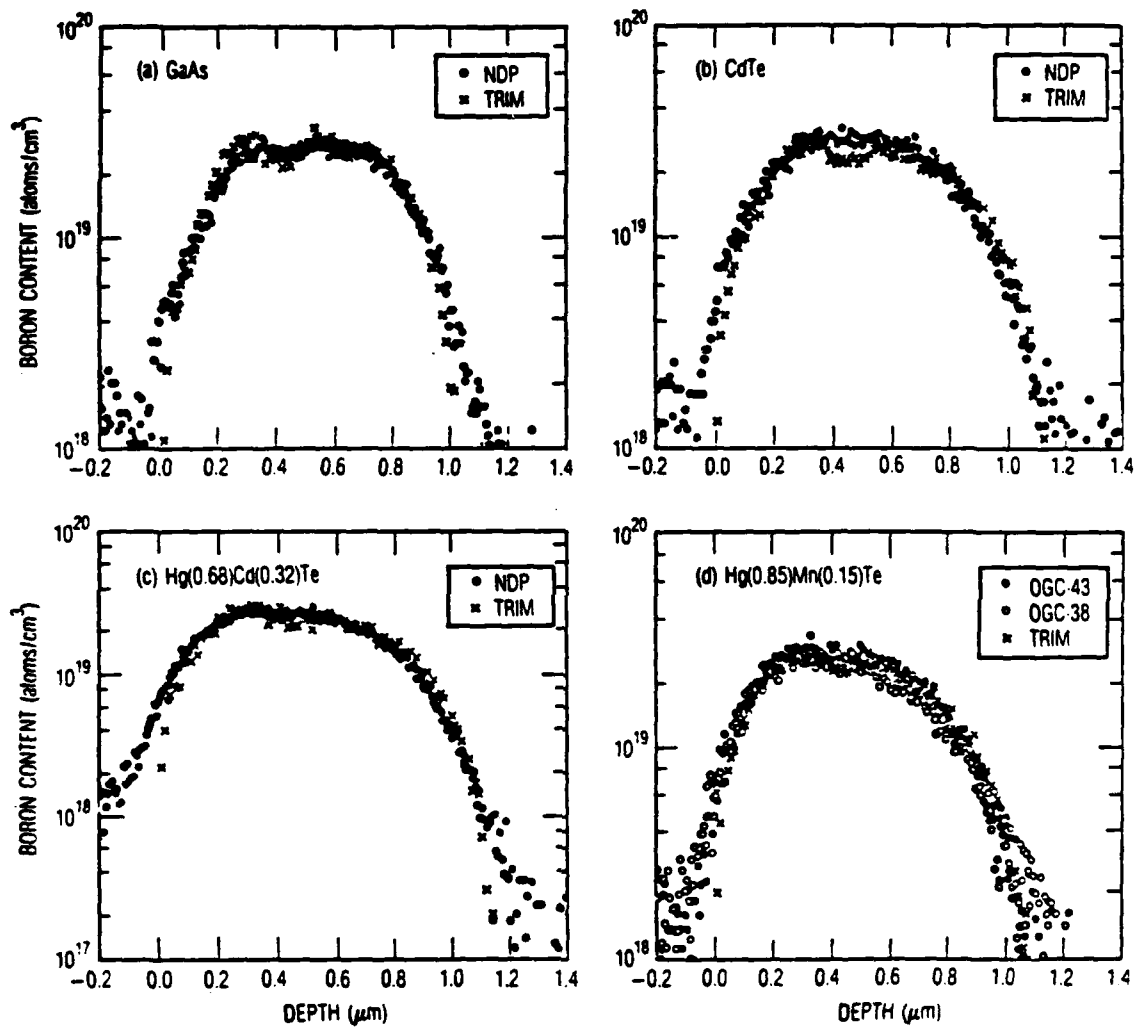


Fig. 2. NDP Profiles From (a) (100)-GaAs, (b) (100)-CdTe, (c) (111)-Hg_{0.68}Cd_{0.32}Te, and (d) Hg_{0.85}Mn_{0.15}Te After Type E Implants. The predicted profiles from the TRIM calculations are also shown.

The influences of thermal anneals that would be representative of conventional electrical activation conditions were examined for some samples. As shown in Fig. 1, essentially no changes in the NDP-measured boron profile were detected from GaAs after 25-min anneals at 850°C under a flowing H₂-Ar atmosphere. A one-hour vacuum anneal (Refs. 6,7) at 499°C of the Type B implanted (111)-CdTe caused the boron profile to shift towards the surface. However, this effect probably arose from the evaporation of about a 25-nm thick layer of surface material during the anneal (Refs. 6,7). The reduction of the "pulse-pile-up" distortion (Ref. 5) from the NDP measurements revealed that some diffusion of the boron had occurred in CdTe during the 500°C anneal as shown by the increased boron content at the deeper regions beyond the peak. However, there was no indication of boron transport in SiO₂-passivated Hg_{0.7}Cd_{0.3}Te crystals (Refs. 5,10) for anneals up to 400°C. Unfortunately, higher annealing temperatures would most likely lead to serious degradation of this material even with protective surface films.

In summary, neutron depth profiling has been found to be a very useful and nondestructive method to monitor the boron contents and ion ranges in several compound semiconductors. More extensive discussions of the effects of boron implants on these materials that include characterizations by electrical, optical, and structural techniques will be presented elsewhere.

REFERENCES

1. P. G. Pitcher, P. L. F. Hemment, and Q. V. Davis, Elect. Lett. **18**, 1090 (1982).
2. M. Berth, M. Cathelin, and G. Durand, Tech. Dig. IEDM 1977, 210.
3. H. Ryssel, K. Mueller, J. Biersack, W. Krueger, G. Lang, and F. Jahnel, Phys. Stat. Sol. (a) **57**, 619 (1980).
4. R. G. Wilson, in Gallium Arsenide and Related Compounds - 1984, edited by B. DeCremoux (Adam Hilger LTD, Bristol, 1985) p. 71.
5. R. C. Bowman, Jr., R. E. Robertson, J. F. Knudsen, and R. G. Downing, Proc. Soc. Photo-Opt. Inst. Eng. **686**, 18 (1986).
6. R. C. Bowman, Jr., R. L. Alt, P. M. Adams, J. P. Knudsen, D. N. Jamieson, and R. G. Downing, J. Cryst. Growth **86**, 768 (1988).
7. R. C. Bowman, Jr., R. G. Downing, and J. F. Knudsen, Trans. Amer. Nucl. Soc. **55**, 212 (1987).
8. J. P. Biersack and L. G. Haggmark, Nucl. Instrum. Methods **174**, 257 (1980).
9. J. F. Ziegler, J. P. Biersack, and U. Littmark, The Stopping and Range of Ions in Solids (Pergamon, New York, 1985).
10. R. C. Bowman, Jr., J. Marks, R. G. Downing, J. F. Knudsen, and G. A. To, Mat. Res. Soc. Symp. Proc. **90**, 279 (1987).

LABORATORY OPERATIONS

The Aerospace Corporation functions as an "architect-engineer" for national security projects, specializing in advanced military space systems. Providing research support, the corporation's Laboratory Operations conducts experimental and theoretical investigations that focus on the application of scientific and technical advances to such systems. Vital to the success of these investigations is the technical staff's wide-ranging expertise and its ability to stay current with new developments. This expertise is enhanced by a research program aimed at dealing with the many problems associated with rapidly evolving space systems. Contributing their capabilities to the research effort are these individual laboratories:

Aerophysics Laboratory: Launch vehicle and reentry fluid mechanics, heat transfer and flight dynamics; chemical and electric propulsion, propellant chemistry, chemical dynamics, environmental chemistry, trace detection; spacecraft structural mechanics, contamination, thermal and structural control; high temperature thermomechanics, gas kinetics and radiation; cw and pulsed chemical and excimer laser development including chemical kinetics, spectroscopy, optical resonators, beam control, atmospheric propagation, laser effects and countermeasures.

Chemistry and Physics Laboratory: Atmospheric chemical reactions, atmospheric optics, light scattering, state-specific chemical reactions and radiative signatures of missile plumes, sensor out-of-field-of-view rejection, applied laser spectroscopy, laser chemistry, laser optoelectronics, solar cell physics, battery electrochemistry, space vacuum and radiation effects on materials, lubrication and surface phenomena, thermionic emission, photo-sensitive materials and detectors, atomic frequency standards, and environmental chemistry.

Computer Science Laboratory: Program verification, program translation, performance-sensitive system design, distributed architectures for spaceborne computers, fault-tolerant computer systems, artificial intelligence, micro-electronics applications, communication protocols, and computer security.

Electronics Research Laboratory: Microelectronics, solid-state device physics, compound semiconductors, radiation hardening; electro-optics, quantum electronics, solid-state lasers, optical propagation and communications; microwave semiconductor devices, microwave/millimeter wave measurements, diagnostics and radiometry, microwave/millimeter wave thermionic devices; atomic time and frequency standards; antennas, rf systems, electromagnetic propagation phenomena, space communication systems.

Materials Sciences Laboratory: Development of new materials: metals, alloys, ceramics, polymers and their composites, and new forms of carbon; non-destructive evaluation, component failure analysis and reliability; fracture mechanics and stress corrosion; analysis and evaluation of materials at cryogenic and elevated temperatures as well as in space and enemy-induced environments.

Space Sciences Laboratory: Magnetospheric, auroral and cosmic ray physics, wave-particle interactions, magnetospheric plasma waves; atmospheric and ionospheric physics, density and composition of the upper atmosphere, remote sensing using atmospheric radiation; solar physics, infrared astronomy, infrared signature analysis; effects of solar activity, magnetic storms and nuclear explosions on the earth's atmosphere, ionosphere and magnetosphere; effects of electromagnetic and particulate radiations on space systems; space instrumentation.